

Maximum allowed solvent accessibilities of residues in proteins

Matthew Tien¹, Austin G. Meyer¹, Stephanie J. Spielman¹, and Claus O. Wilke^{1*}

Address:

¹Section of Integrative Biology, Institute for Cellular and Molecular Biology, and Center for Computational Biology and Bioinformatics. The University of Texas at Austin, Austin, TX 78731, USA.

*Corresponding author

Email: wilke@austin.utexas.edu

Phone: +1 512 232 2459

Manuscript type: research article

Keywords: solvent accessibility, relative solvent accessibility, tripeptide, hydrophobicity scale

Abstract

The relative solvent accessibility (RSA) of a residue in a protein measures the extent of burial or exposure of that residue in the 3D structure. RSA is frequently used to describe a protein's biophysical or evolutionary properties. To calculate RSA, a residue's solvent accessibility (SA) needs to be normalized by a suitable reference value for the given amino acid; several normalization scales have previously been proposed. However, these scales do not provide tight upper bounds on SA values frequently observed in empirical crystal structures. Instead, they underestimate the largest allowed SA values, by up to 20%. As a result, many empirical crystal structures contain residues that seem to have RSA values in excess of one. Here, we derive a new normalization scale that does provide a tight upper bound on observed SA values. We pursue two complementary strategies, one based on extensive analysis of empirical structures and one based on systematic enumeration of biophysically allowed tripeptides. Both approaches yield highly congruent results that consistently exceed published values. We conclude that previously published SA normalization values were too small primarily because the conformations that maximize SA had not been correctly identified. Finally, we show that empirically derived hydrophobicity scales are sensitive to accurate RSA calculation, and we derive a hydrophobicity scale that shows excellent agreement with experimentally measured scales.

1 Introduction

Relative solvent accessibility (RSA) has emerged as a commonly used metric describing protein structure in computational molecular biology, with the particular application of identifying buried or exposed residues. It is defined as a residue’s solvent accessibility (SA) normalized by a suitable maximum value for that residue. RSA was first introduced in the context of hydrophobicity scales derived by computational means from protein crystal structures [1–5]. More recently, RSA has been shown to correlate with protein evolutionary rates and has been incorporated as a parameter into models which determine these rates [6–13]. As RSA straightforwardly characterizes the local environment of residues in proteins structure, many studies have developed computational methods to predict RSA from protein primary and/or secondary structure [14–17]. Further applications of RSA include identification of surface, interior, and interface regions in proteins [18], protein-domain prediction [19], and prediction of deleterious mutations [20].

To derive a residue’s RSA from its surface area, an SA normalization factor is needed for each amino acid. By convention, these normalization values have been derived from evaluating the surface area around a residue of interest X when placed between two glycines, to form a Gly- X -Gly tripeptide. Most commonly, the normalization values utilized are those previously described by either Rose et al. [2] or by Miller et al. [3]. The primary distinction between these two sets of normalization values lies in the different ϕ and ψ dihedral backbone angles chosen when evaluating Gly- X -Gly tripeptide conformations. Rose et al. [2] considered tripeptides with backbone angles representing an average of observed ϕ and ψ angles, whereas Miller et al. [3] considered tripeptides in the extended conformation ($\phi = -120^\circ$, $\psi = 140^\circ$).

However, as these SA normalization values are being applied to residues in an increasing numbers of empirically determined 3D protein crystal structures, one finds that neither the Rose [2] nor the Miller [3] scale accurately identifies the true upper bound for a residue’s SA. In fact, virtually all amino acids display, on occasion, SA values in excess of the normalization SA values provided by either scale. Some do so quite frequently (e.g. R, D, G, K, P), reaching RSA values of up to 1.2. This discrepancy, which leads to RSA values > 1 , is generally known in the field though rarely acknowledged in print.

Here, we derive a new set of SA normalization values that provide a tight upper bound on SA values observed in biophysically realistic tripeptide conformations. To calculate these normalization values, we pursue two complementary strategies—one empirical and one theoretical. For the empirical approach, we mined thousands of 3D crystal structures and recorded the maximum SA values we found for each amino acid across all structures. For the theoretical approach, we computationally built Gly- X -Gly tripeptides and systematically evaluated all biophysically allowed conformations to determine a maximum theoretical SA value. These two strategies yield highly congruent results and ultimately produce comparable normalization scales that tightly bound SA for all 20 amino acids. We then return to the historic motivation for RSA and investigate the implications of our results for hydrophobicity scales. We find that both SA normalization and non-normal distribution of RSA values affect the performance of empirically derived hydrophobicity scales. We propose a new scale that correlates with $r > 0.8$ with experimentally derived hydrophobicity scales.

2 Results

2.1 Published SA normalization values are too small

We initially assessed the accuracy of Rose’s [2] and Miller’s [3] SA normalization scales through an exhaustive survey of the SA values found in experimentally determined protein structures. We obtained a list of 2908 high-quality PDB structures from the PISCES server [21]. We then calculated SA for each residue in all 2908 structures, excluding any chain-terminating residues. SA values were subsequently normalized using the scales of either Rose et al. [2] or Miller et al. [3], to obtain RSA. For either scale and each amino acid, we found that residues with $RSA > 1$ were not uncommon (Figure 1); RSA values exceeded unity by up to 20%. The amino acids that most commonly displayed $RSA > 1$ were R, D, G, K, P. For those amino acids, RSA values >1 occurred at frequencies of 1% to 3% of all residues, depending on the normalization scale used (Figure 1).

To determine the underlying factors leading to $RSA > 1$, we examined the association between RSA and the following factors: residue neighbors, secondary structure, bond lengths, bond angles, and dihedral angles. For most of these quantities, we found no strong association with RSA (not shown). We did, however, find a clear association with residues’ ϕ and ψ backbone angles. For example, consider the Ramachandran plot of alanine (Figure 2). A noticeable cluster of high-RSA residues falls into the α -helix region of $\phi \approx -50$, $\psi \approx -45$. We found similar results for other amino acids (not shown). Importantly, neither Rose nor Miller derived their normalization SA values in that region of backbone angles. Therefore, we concluded that previous SA normalization scales were obtained with poorly chosen ϕ and ψ angles.

2.2 Modeling Tripeptides Yields Significantly Higher Maximum SA Values

To derive maximum SA values for each amino acid X, we computationally constructed Gly-X-Gly tripeptides and systematically rotated them through all biophysically allowed conformations (see Supporting Text for details.) When constructing the tripeptides, we set bond lengths and angles (excluding ω , ϕ , ψ , and χ angles) for each amino acid equal to the average values observed for that amino acid in our reference set of 2908 PDB structures. We set $\omega = 180^\circ$. We then rotated the ϕ and ψ around the X residue in discrete 1° steps, exhaustively enumerating all conformations except those nonexistent or rare in actual crystal structures. Additionally, we iterated through all rotamer angles χ that were sterically possible with each (ϕ, ψ) combination. For those amino acids with more than 10 possible distinct rotamer conformations, as determined by the Dunbrack database [21], we evaluated ten randomly chosen rotamer conformations. We recorded the maximum SA observed for each (ϕ, ψ) backbone-angle combination.

Next, we compared the resulting theoretical maximum SA values to the empirically observed maximum SA values. We binned both the theoretical and the empirical values into discrete $5^\circ \times 5^\circ$ bins of (ϕ, ψ) and recorded the maximum SA in each bin. To eliminate nonexistent or rare conformations, we discarded for both data sets all bins that contained fewer than five observations in the empirical data set. We displayed the remaining data in

side-by-side Ramachandran plots (Figure 3) and generally found good congruence between the theoretical and the empirical values for all amino acids. Regions that had the highest maximum SA in the theoretical data set also had the highest maximum SA in the empirical data set. The highest SA values were generally observed in the α -helix region of the Ramachandran plot (Figure 3). Based on these results, we propose new maximally exposed geometries for each amino acid (Table S1).

We further evaluated our model’s performance by directly comparing theoretical and empirical maximum SA values in each (ϕ, ψ) bin. We calculated the difference between these two values for each $5^\circ \times 5^\circ$ bin (now including all bins with at least one observation in the empirical data set). We then plotted this difference against the number of empirical observations obtained for each bin (Figure 4). We found that with increasing amounts of empirical data, this difference approached zero; the maximum SA values from both approaches converged as more data was available. Moreover, even for sparsely populated bins, at least some bins showed a difference near zero, regardless of the number of observations in each bin. Therefore, while our results did improve with increasing amounts of data, they were also largely robust to smaller data sets. The overall maximum SA values for each amino acid as derived from both approaches are summarized in Table 1. These maximum values were again derived excluding bins with fewer than five empirical observations.

2.3 Application to Empirically Derived Hydrophobicity Scales

A long-standing problem in protein biochemistry has been the disagreement between empirically derived and experimentally measured hydrophobicity scales. Here, we use the term “empirically derived” to describe any hydrophobicity measure obtained by evaluating how frequently different amino acids occur in the core or near the surface of empirically determined protein crystal structures. By contrast, “experimentally measured” applies to hydrophobicity measures obtained by direct experimental observation of amino-acid behavior in suitable chemical environments, such as in water/vapor solutions [22]. One would expect that empirically derived and experimentally measured hydrophobicity scales should largely agree, yet there are striking discrepancies between the most commonly used empirical scale, the Rose scale [2], and the two most commonly used experimental scales, the Wolfenden scale [22] and the Kyte–Doolittle scale [23] (Figure 5, left column).

Rose et al. [2] derived their hydrophobicity scale by evaluating the mean RSA for each amino acid across a set of reference crystal structures. Hence, we asked whether repeating this calculation but using our improved SA normalization values would yield an improved scale. Indeed, we found that mean RSA calculated using our methods correlated better with both the Wolfenden and the Kyte–Doolittle scales than the Rose scale did (Figure 5, middle column). However, improvements were modest; correlation coefficients rose from $r = 0.61$ to $r = 0.70$ for the Wolfenden scale and from $r = 0.84$ to $r = 0.89$ for the Kyte–Doolittle scale (Table 2).

Encouraged by this improvement, we next investigated whether other improvements in the empirical scale could be made. We specifically considered improvements only in the statistical procedure of deriving the scale, without abandoning the overall philosophy of assessing the relative frequencies of amino acids in the core or near the surface of empirical protein structures. One obvious place for improvement was to replace mean RSA by a

different measure of center of the RSA distributions. The distributions of RSA values per amino acid tend to be highly skewed (see for example Figure S1), and thus mean RSA does not accurately reflect the most common RSA values. Skewed distributions are common in many statistical applications, and conventional approaches to analyzing such distributions are to calculate the median instead of the mean or to transform the data before calculating the mean.

We evaluated a number of alternatives to mean RSA, including median RSA and various transformation methods. We found that most alternatives yielded further improvements in the empirical hydrophobicity scale (not shown). Most importantly, though, we noticed that the improvements grew larger as more emphasis was placed on the relative fraction of completely buried residues ($\text{RSA} = 0$) of a given amino acid. This observation prompted us to consider the fraction of completely buried residues as a hydrophobicity scale. (In 1976, Chothia et al. [1] had already pursued a similar approach, with the limited data available at the time.) We found that this empirical hydrophobicity scale displayed much higher correlations with the experimental scales than did the scales derived from mean RSA (Figure 5). Correlation coefficients were now $r = 0.83$ for the Wolfenden scale and $r = 0.96$ for the Kyte–Doolittle scale (Table 2). In fact, the Kyte–Doolittle scale was virtually identical to the fraction of completely buried residues. We also considered the fraction of 95% buried residues ($\text{RSA} < 0.05$) and found that the correlation with the Kyte–Doolittle scale was again $r = 0.96$ but the correlation with the Wolfenden scale was only $r = 0.79$ (Table 2).

We conclude that there is no substantive difference between empirically derived and experimentally measured hydrophobicity scales. Apparent differences in prior work were caused by technical limitations, specifically by insufficiently large SA normalization values (making all residues appear more exposed than they actually are) and by a statistical approach giving highly exposed residues undue weight (making the fraction of exposed residues appear larger than it actually is).

3 Discussion

We have derived significantly improved SA normalization values. Our normalization values provide a tight upper bound to the largest observed SA values in empirical structures. By contrast, previously published SA normalization values were too small, by up to 20%, and frequently led to RSA values > 1 . We estimated the maximum allowed SA for each amino acid by computationally modeling Gly-X-Gly tripeptides, where X is the amino acid of interest, and exhaustively surveying SA over all biophysically feasible conformations. We found that maximally exposed conformations tend to fall into the α -helix region of Ramachandran plots, and that extended conformations display some side-chain burial. The results of our modeling approach were consistent with maximum SA values found by surveying nearly 3000 empirical protein crystal structures. We also revisited the problem of deriving a hydrophobicity scale from empirical protein structures. We found that substantial improvements could be made over previous scales that were built on the mean RSA for each amino acid. Our best-performing scale, which measures simply the fraction of times each amino acid occurs in a fully buried conformation, is highly correlated with two widely used experimental scales and is nearly identical to one of them.

Our method of obtaining SA normalization values was similar to those of Rose et al. [2] and of Miller et al. [3]. Rose et al. [2] calculated their SA normalization values by computing the SA of residue X in Gly-X-Gly tripeptides whose conformations were chosen based on the average dihedral angles from available empirical data at the time. Miller et al. [3], on the other hand, calculated their SA normalization values by computing the SA of an extended trimer structure with $\phi = -120^\circ$, $\psi = 140^\circ$ and with side-chain conformations that were frequently observed in the empirical data. The key distinction between these previous approaches and ours lies in our exhaustive sampling of tripeptide conformations. By modeling all biophysically feasible discrete combinations of ϕ and ψ angles and varying rotamers, we identified the ideal conformations which yield maximum allowed SA. To pursue our modeling strategy, we developed a program that allowed us to easily construct peptide chains from scratch in arbitrary conformations (see Supporting Text for details).

Our theoretical modeling approach to exhaustively survey tripeptides has two potential shortcomings. First, for bond lengths and angles (except major dihedral angles), we used mean values observed in a large number of protein crystal structures. This approach neglects the variation around the mean, and there could be rare cases where unusually large bond lengths or unusual bond angles might cause SA to become larger than estimated here. Such scenarios would have to be exceedingly rare, however, since we did not find a single case in which the largest empirically derived maximum SA value exceeded the largest theoretically derived maximum SA value (Table 1). Second, for amino acids with more than 10 distinct rotamer conformations, we did not exhaustively enumerate all possible conformations but only sampled 10 conformations at random. Thus, in principle it is possible that we missed a particular rotamer conformation that would have corresponded to a larger SA value than the maximum we observed. Two arguments suggest that this issue is not likely a major source of error. First, again, we did not find a single case in which the empirical maximum SA was larger than the theoretical maximum SA. Second, maximum SA varied slowly with ϕ and ψ , and by exhaustively enumerating conformations in 1° steps, in effect we sampled the most exposed conformations multiple times, thus reducing the chance of missing a rare, large-SA conformation.

As RSA calculations are based on the Gly-X-Gly framework, we excluded all chain terminating residues from both the empirical and the theoretical analysis. Even with our improved SA normalization values, then, chain-terminating residues may still display $\text{RSA} > 1$. We therefore recommend that future analyses making use of RSA similarly exclude any chain-terminating residues, as their RSA estimates will not be precise. Suitable normalization values for chain-terminating residues are not available at present.

The comparison between experimental and empirically derived hydrophobicity scales has been a persistent problem in biochemistry. Resolving the discrepancies between empirically-derived data and experimentally derived thermodynamics of hydrophobicity could provide crucial insight into algorithms of protein-structure prediction and de-novo protein folding. Wolfenden et al. [22] was the first to propose an approach for reconciling both approaches by correlating the distribution of amino acid exposure with their experimental behaviors in water/vapor solutions. More recently, Moelbert et al. [4] attempted to reconcile these disparities by correlating hydrophobic states with surface-exposure patterns of protein structures. Additionally, Shaytan et al. [5] assessed the distribution of amino acid exposure in proteins to discern apparent free energies of transfer between protein interior and surface states, and

found that free energy is highly correlated with experimental hydrophobicity scales [5]. Each of these approaches used the SA normalization values from Rose et al. [2] or Miller et al. [3]. Since the normalization SA values developed here are more accurate, we believe that our findings are noteworthy in determining exposure states. Further, we would like to emphasize that experimental and empirical scales are much more similar than has been commonly thought, as long as the correct empirical measure (fraction of buried residues) is employed. Note, however, the Kyte–Doolittle scale [23] may be highly correlated with the fraction of buried residues in part because Kyte and Doolittle incorporated into their scale side-chain burial information from a limited number of protein structures known at the time [23]. Hence, of the two scales used here for comparison, only the Wolfenden scale [22] can be considered a truly independent experimental verification of our proposed empirical scale.

In summary, we have presented significantly improved SA normalization values and an empirically derived hydrophobicity scale that correlates highly with experimental scales. We recommend that our theoretical normalization values (column 1 of Table 1) be used to normalize SA, and that fraction of 100% buried residues (column 1 of Table 3) be used as empirical hydrophobicity scale.

4 Materials and Methods

We obtained a set of 2908 high-quality protein crystal structures using the PISCES server [21]. We imposed the following requirements: resolution of 1.8 Å or less, an R -free value < 0.25 , and a pairwise mutual sequence identity of at most 20%. For each amino-acid residue in all 2908 structures, we retrieved bond lengths, bond angles, dihedral angles, peptide bond lengths, and nearest neighbors. Chain-terminating residues, defined as those residues whose peptide bond lengths with any neighboring residue was greater than six standard deviations from the protein’s mean peptide bond length, were excluded from all subsequent analyses.

We used the program DSSP (2011 version) [24] to calculate solvent accessibility (SA) and to identify the secondary structure of each residue across all proteins. We calculated RSA as $RSA = SA / \text{Maximum SA}$, where “Maximum SA” corresponds to the maximum SA value, as determined by the normalization scale used, for the focal amino acid.

We developed a novel procedure to computationally build Gly-X-Gly tripeptide structures from scratch. This method is described in detail in Supporting Text. Briefly, we first constructed peptides in a defined conformation by placing each atom at the correct position in 3D space. We then adjusted ϕ , ψ , and χ angles to obtain the desired conformation.

5 Acknowledgments

This work was supported by NIH grant R01 GM088344 to C.O.W. We thank Dariya Sydykova for help with the python code used to build model tripeptides.

References

- [1] Chothia C (1976) The nature of the accessible and buried surfaces in proteins. *J Mol Biol* :1–14.
- [2] Rose GD, Geselowitz AR, Lesser GJ, Lee RH, Zehfus MH (1985) Hydrophobicity of amino acid residues in globular proteins. *Science* 229:834–838.
- [3] Miller S, Janin J, Lesk AM, Chothia C (1987) Interior and surface of monomeric proteins. *J Mol Biol* 196:641–656.
- [4] Moelbert S, Emberly E, Tang C (2004) Correlation between sequence hydrophobicity and surface-exposure pattern of database proteins. *Prot Sci* :752–762.
- [5] Shaytan AK, Shaitan KV, Khokhlov AR (2009) Solvent accessuvke surface area of amino acid residues in globular proteins: Correlations of apparent transfer free engergies with experimental hydrophobicity scales. *Biomacromolecules* :1224–1237.
- [6] Goldman N, Thorne JL, Jones DT (1998) Assessing the impact of secondary structure and solvent accessibility on protein evolution. *Genetics* 149:445–458.
- [7] Bloom JD, Drummond DA, Arnold FH, Wilke CO (2006) Structural determinants of the rate of protein evolution in yeast. *Mol Biol Evol* 23:1751–1761.
- [8] Franzosa EA, Xia Y (2009) Structural determinants of protein evolution are context-sensitive at the residue level. *Mol Biol Evol* 26:2387–2395.
- [9] Zhou T, Weems M, Wilke CO (2009) Translationally optimal codons associate with structurally sensitive sites in proteins. *Mol Biol Evol* 26:1571–1580.
- [10] Franzosa EA, Xia Y (2012) Independent effects of protein core size and expression on structure-evolution relationships at the residue level. *PLoS One* 7:e46602.
- [11] Scherrer MP, Meyer AG, Wilke CO (2012) Modeling coding-sequence evolution within the context of residue solvent accessibility. *BMC Evol Biol* 12:179.
- [12] Meyer AG, Wilke CO (2012) Integrating sequence variation and protein structure to identify sites under selection. *Mol Biol Evol*, in press.
- [13] Contant GC, Stadler PF (2009) Solvent exposure imparts similar selective pressures across a range of yeast proteins. *Mol Biol Evol* 26:1155–1161.
- [14] Rost B, Sander C (1994) Conservation and prediction of solvent accessibility in protein families. *Proteins* 20:216–226.
- [15] Pollastri G, Baldi P, Fariselli P, Casadio R (2002) Prediction of coordination number and relative solvent accessibility in proteins. *Proteins* 47:142–153.
- [16] Kim H, Park H (2004) Prediction of protein relative solvent accessibility with support vector machines and long-range interaction 3D local descriptor. *Proteins* 54:557–562.

- [17] Nguyen MN, Rajapakse JC (2005) Prediction of protein relative solvent accessibility with a two-stage SVM approach. *Proteins* 59:30–37.
- [18] Levy ED (2010) A simple definition of structural regions in proteins and its use in analyzing interface evolution. *J Mol Biol* 403:660–670.
- [19] Cheng J, Sweredoski MJ, Baldi P (2006) DOMpro: protein domain prediction using profiles, secondary structure, relative solvent accessibility, and recursive neural networks. *Data Mining and Knowledge Discovery* 13:1–10.
- [20] Chen H, Zhou HX (2005) Prediction of solvent accessibility and sites of deleterious mutations from protein sequence. *Nucl Acids Res* 33:3193–3199.
- [21] Wang G, Dunbrack RL (2003) PISCES: a protein sequence culling server. *Bioinformatics* 19:1589–1591.
- [22] Wolfenden R, Anderson L, Cullis PM, Southgate CCB (1981) Affinities of amino acid side chains for solvent water. *Biochemistry* :849–855.
- [23] Kyte J, Doolittle RF (1982) A simple method for displaying the hydropathic character of a protein. *J Mol Biol* 157:105–132.
- [24] Kabsch W, Sander C (1983) Dictionary of protein secondary structure: pattern recognition of hydrogen-bonded and geometrical features. *Biopolymers* 22:2577–2637.

Table 1: Proposed values for SA normalization (in \AA^2), compared to previously used scales defined by Rose et al. [2] and Miller et al. [3].

Residue	Theoretical	Empirical	Miller (1987)	Rose (1985)
Alanine	129.0	121.0	113.0	118.1
Arganine	274.0	265.0	241.0	256.0
Asparagine	195.0	187.0	158.0	165.5
Aspartate	193.0	184.0	151.0	158.7
Cysteine	158.0	140.0	140.0	146.1
Glutamine	224.0	215.0	189.0	193.2
Glutamate	223.0	215.0	183.0	186.2
Glycine	104.0	98.0	85.0	88.1
Histidine	209.0	208.0	194.0	202.5
Isoleucine	197.0	195.0	182.0	181.0
Leucine	201.0	192.0	180.0	193.1
Lysine	237.0	227.0	211.0	225.8
Methionine	218.0	203.0	204.0	203.4
Phenylalanine	239.0	228.0	218.0	222.8
Proline	159.0	159.0	143.0	146.8
Serine	151.0	143.0	122.0	129.8
Threonine	172.0	161.0	146.0	152.5
Tryptophan	282.0	265.0	259.0	266.3
Tyrosine	263.0	255.0	229.0	236.8
Valine	174.0	165.0	160.0	164.5

Table 2: Correlation coefficients r between experimental hydrophobicity scales [22, 23] and empirical hydrophobicity scales (Rose et al.’s scale [2] and scales created in our analyses). “Mean RSA (empirical)” is a scale in which RSA was calculated using empirical normalization values (Table 1), while “Mean RSA (theoretical)” is the same but using theoretical normalization values (Table 1).

Scale	Wolfenden scale		Kyte–Doolittle scale	
	r	P value	r	P value
Rose	0.614	0.0040	0.841	3.4×10^{-06}
Mean RSA (empirical)	0.687	8.1×10^{-04}	0.886	2.0×10^{-07}
Mean RSA (theoretical)	0.699	6.0×10^{-04}	0.890	1.5×10^{-07}
95% Buried	0.786	4.1×10^{-05}	0.956	5.1×10^{-11}
100% Buried	0.830	5.8×10^{-06}	0.956	4.6×10^{-11}

Table 3: Fraction of times a given amino acid is found in a buried conformation. 100% buried residues have RSA = 0 (corresponding to SA < 1Å) and 95% buried residues have RSA < 0.05.

Amino Acid	Fraction 100% Buried	Fraction 95% Buried
Alanine	0.223	0.394
Arginine	0.0109	0.0694
Asparagine	0.0445	0.142
Aspartate	0.0274	0.102
Cysteine	0.273	0.539
Glutamate	0.0169	0.0663
Glutamine	0.0264	0.104
Glycine	0.162	0.286
Histidine	0.0509	0.186
Isoleucine	0.239	0.509
Leucine	0.207	0.478
Lysine	0.00596	0.0275
Methionine	0.211	0.45
Phenylalanine	0.185	0.477
Proline	0.0583	0.16
Serine	0.0989	0.23
Threonine	0.0984	0.237
Tryptophan	0.0937	0.358
Tyrosine	0.08	0.303
Valine	0.247	0.488

Table S1. Backbone conformation of maximally exposed trimer structures. Multiple rows per residue indicate alternative conformations with comparable solvent exposure.

Residue	Empirical		Theoretical	
	ϕ	ψ	ϕ	ψ
Alanine	-51.9°	-37.9°	-60°	-15°
	-66.7°	-13.1°	-45°	-40°
	-52.1°	-33.6°	70°	-5°
	-58.6°	-30.7°		
Arginine	-79.2°	-20.2°	-70°	-25°
			-70°	-5°
			-60°	-15°
			-55°	-30°
Asparagine	-74.1°	-3.6°	-40°	-50°
	-94.8°	-3.4°	-50°	-40°
	-67.4°	-16.8°	70°	-30°
			70°	-5°
Aspartate	-73.0°	-11.0°	70°	-5°
Cysteine	-61.4°	-23.4°	-60°	-20°
Glutamine	-66.8°	-20.3°	-60°	-15°
			70°	-5°
Glutamate	-60.2°	-39.6°	-60° to -55°	-25° to -20°
			60°	15°
			65°	5°
Glycine	76.9°	0.7°	-65° to -60°	-15° to -10°
Histidine	-93.7°	12.9°	-80° to -75°	130°
			-80°	170°
Isoleucine	-64.1°	-21.9°	-55°	-25°
			-50°	-40°
Leucine	-58.1°	-24.8°	-70°	-5°
			55°	15°
Lysine	-62.1°	-24.4°	-60°	-15°
Methionine	-67.5°	-27.5°	-60°	-20°
			-55°	-30°
Phenylalanine	-50.3°	135.2°	-45°	-45°
Proline	-38.3°	-57.8°	-55°	-20°
			-40°	-50°
Serine	-58.1°	-27.3°	-60° to -55°	-25° to -15°
			65°	5°
			70°	-5°
Threonine	-103.4°	1.1°	-60°	-15°
			-45°	-45°
Tryptophan	-67.6°	-9.8°	-75°	-15°
			-75°	0°
			-60° to -55°	-25° to -20°
			-50°	-40° to -35°
Tyrosine	-61.7°	-32.4°	-50°	-40° to -35°
Valine	-48.9°	-28.0°	-55°	-25°

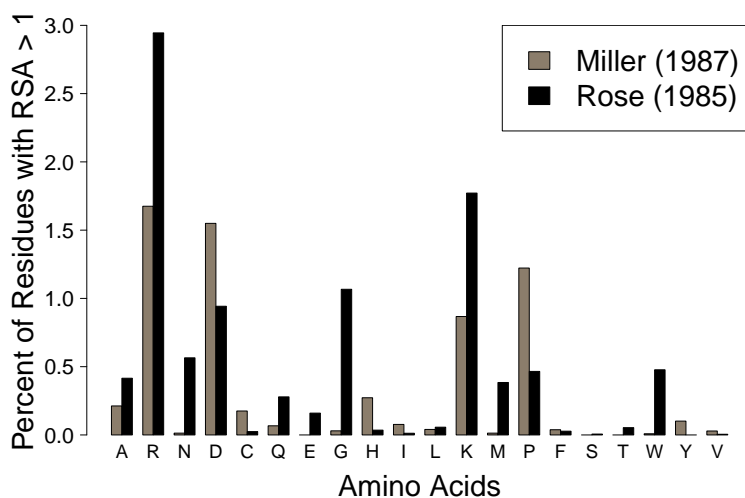


Figure 1: Frequency of residues with $RSA > 1$ in empirical protein structures. Nearly all amino acids, and notably R, D, K, G, and P, show $RSA > 1$ when RSA is calculated using the normalization values of either Rose et al. [2] or Miller et al. [3].

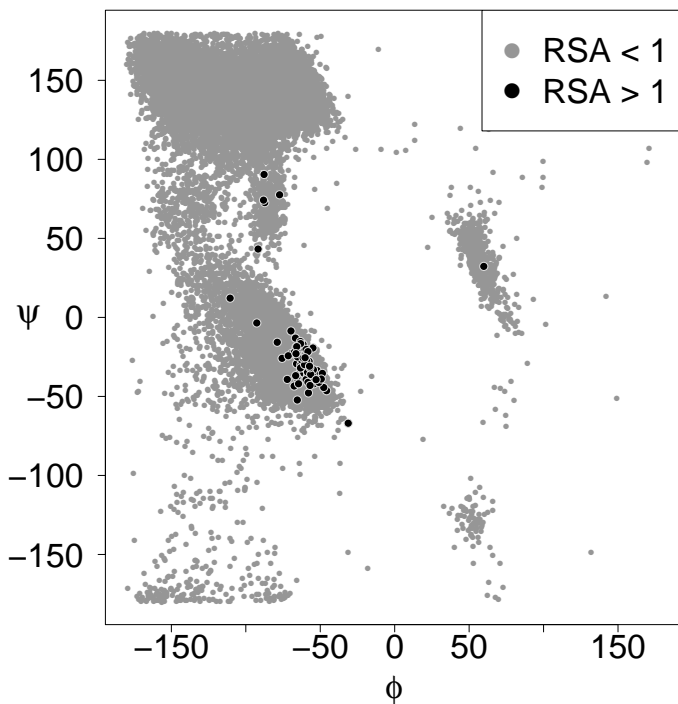


Figure 2: Ramachandran plot for alanine residues in our empirical data set. Coordinates which correspond to RSA values > 1 are shown in black and are clearly concentrated around coordinates $(-50^\circ, -45^\circ)$. We therefore propose that this region contains the maximally exposed conformation of alanine and should be used for calculating maximum SA.

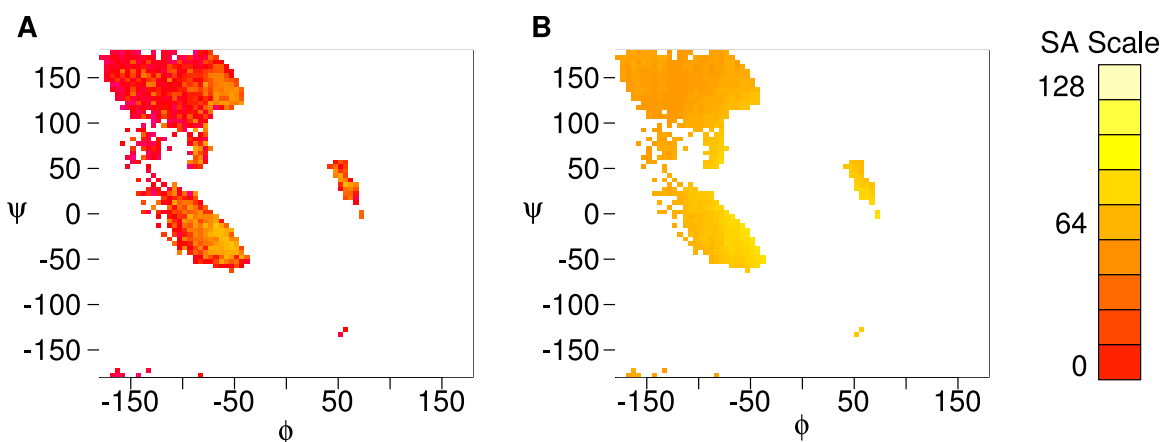


Figure 3: Ramachandran plots for empirical and theoretical maximum SA values of alanine. (A) Empirical maximum SA values for each 5° by 5° bin. Only bins which contained at least five observations are shown. (B) Theoretical maximum SA values, as determined by computational modeling, shown for non-empty bins in (A). Both the empirical and the theoretical approach find the largest SA values in the α -helix region around $(-50^\circ, -45^\circ)$. By contrast, the extended conformation $(-120^\circ, 140^\circ)$ leads to relatively low maximum SA.

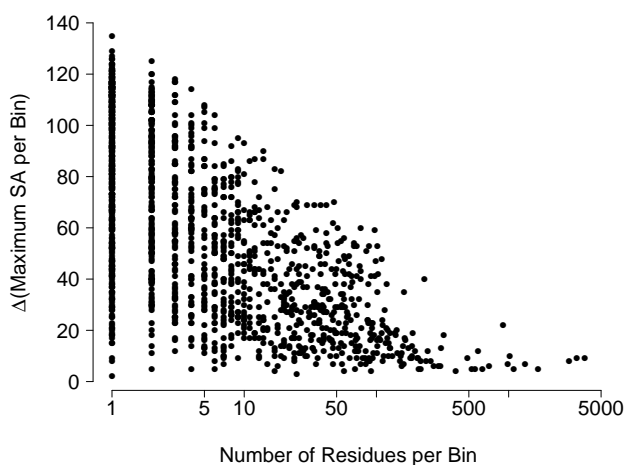


Figure 4: Difference between theoretically and empirically determined maximum SA values for alanine, across 5° by 5° bins. As the amount of data per bin increases, the difference between theoretical and empirical maximum SA approaches zero, demonstrating that our two methods converged with increasing amounts of data. Furthermore, the difference between values is frequently zero, even when little data is available for a bin. This observation indicates that our theoretically derived maximum SA values provide a tight bound on the empirically observed ones.

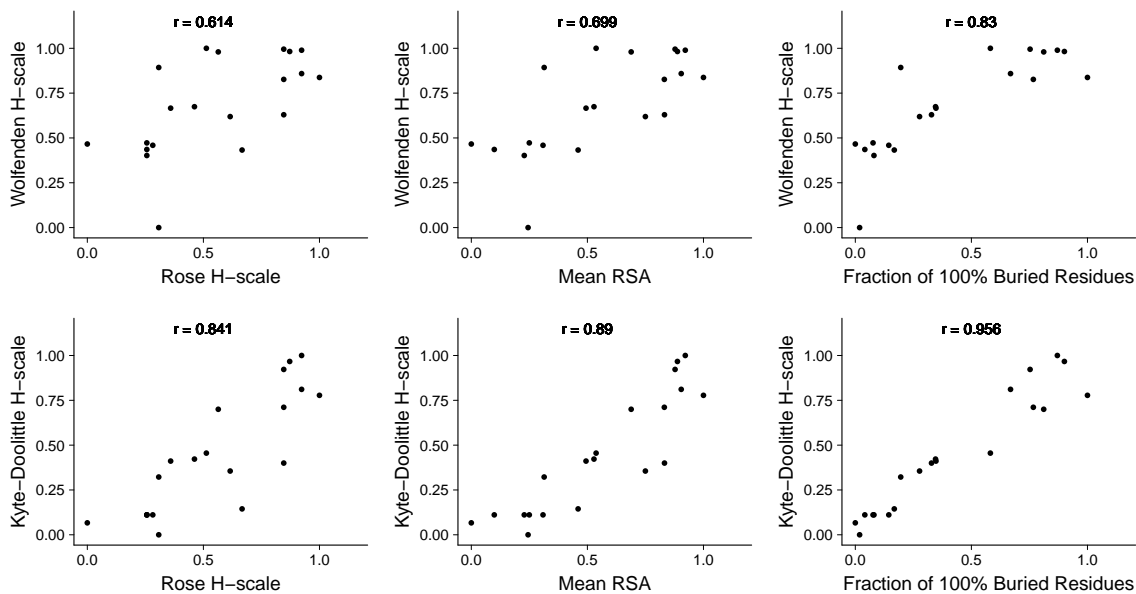


Figure 5: Correlation between experimentally measured and empirically derived hydrophobicity scales. The top row of graphs shows the Wolfenden experimental scale [22] plotted against (i) the Rose scale [2], (ii) our mean-RSA scale, and (iii) our scale measuring the fraction of 100% buried residues. The second row shows the same information but for the Kyte–Doolittle scale [23]. We used theoretical maximum SA values for scales (ii) and (iii); all hydrophobicity scales were standardized to fall between 0 and 1. Our mean-RSA scale performs slightly better than the Rose scale. However, the fraction of 100% buried residues clearly outperforms both scales built on mean RSA.

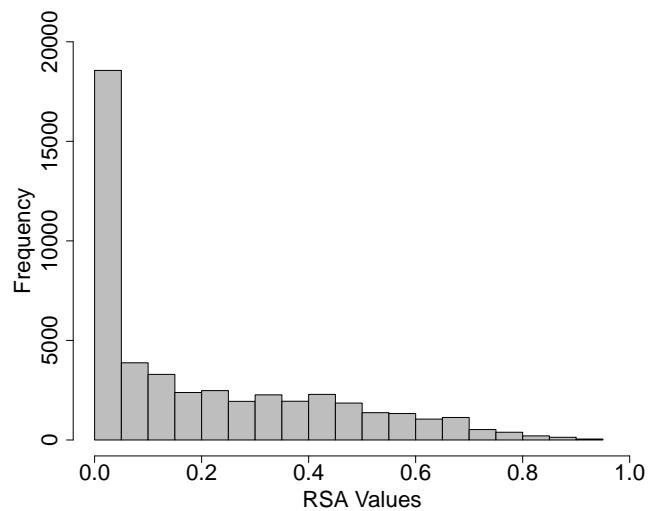


Figure S1. Distribution of RSA values for alanine. RSA was calculated using our theoretically determined normalization values. This distribution is highly non-normal with a strong right skew. Therefore, mean RSA is a poor measure of center for this distribution. Similarly skewed distributions are found for most amino acids (not shown).